Demonstration of Multi-channel Optical Interconnection using Imaging Fiber Bundles Butt Coupled to Optoelectronic Circuits

Donald M. Chiarulli, Steven P. Levitan, Paige Derr, and Robert Hofmann

University of Pittsburgh, Pittsburgh, PA 15260

Bryan Greiner and Matt Robinson

Schott Fiber Optics, 122 Charlton Street, Southbridge, MA 01550-1960

OCIS Codes: 060.0060; 060.2350; 200.4650; 250.3140; 060.1810; 130.3120

ABSTRACT

In the five experiments described in this paper we demonstrate and characterize the basic functionality of imaging fiber bundles for optoelectronic chip level interconnections. We demonstrate the transmission of spot arrays with spot sizes and spot pitch roughly equal to two and four times the core pitch respectively. We show that optoelectronic integrated circuits, including sources and detectors, can be directly butt coupled to fiber bundles without any additional optical elements. We demonstrate a 16 channel interconnect with –23db of crosstalk and we characterize the most significant optical loss mechanism. Finally, we show how imaging fiber bundles can be used to implement more complex interconnection structures by an example of a hybrid bonded structure that implements a low cost, high connectivity, solution for more advanced system architectures.

Introduction

Recent advances in optoelectronic (OE) devices and in processing technology have focused attention on the packaging of multi-chip optoelectronic systems. Alignment tolerances and geometrical restrictions often make the implementation of free space optics within these systems quite difficult. Critical alignment issues also characterize fiber-per-channel guided wave systems based optical ribbon cable or large core fiber arrays. In this paper, we present an alternative packaging technology based on imaging fiber bundles. In an imaging fiber bundle, each optical data channel is carried by multiple fibers. An array of spots imaged at one end of the fiber bundle is correspondingly imaged on the opposite end. In this manner, imaging fiber bundles are capable of supporting the spatial parallelism of a free space interconnect with relaxed alignment and geometry constraints.

Fiber bundles can be used in OE systems to directly connect pairs of OE integrated circuits or they may connect subsets of optical elements on each chip for routing and distribution of the channels. As we demonstrate in this paper, they can be directly coupled to OE chips without additional optical elements. Moreover, hybrid configurations, produced by bonding multiple bundles in various configurations[1], can implement fan-in and fan-out structures such as parallel optical passive stars (POPS) [2] and spatial switching structures such optical cross-bar networks [3].

In this paper we present the results of a series of experiments which were designed to test and characterize the performance of imaging fiber bundles for chip level interconnection of optoelectronic VLSI devices. After a brief description of the technology in the next section, we report on this series of experiments. In the first, we tested the resolution of dense spot arrays for spot pitch on the order of twice the core spacing. In the second, we tested the coupling properties for fiber image guides butt coupled to a VCSEL array source. In the third experiment, a functioning multi-channel interconnect was tested by butt coupling each end of the fiber bundle to a VCSEL array and detector array respectively. Channel crosstalk was also characterized in this experiment. In a fourth experiment, we tested the contributions to overall power budget of various power loss mechanisms and measured loss uniformity over the surface of a bundle. In our fifth and final experiment we tested a key spatial switch element that is the basis for a multi-point interconnection architecture based on imaging fiber bundles. Taken as a group these experiments demonstrate that imaging fiber bundles are an efficient and cost effective packaging technology for OE systems.

Imaging Fiber Bundle Technology

The imaging fiber bundles descibed in this paper are fiber image guides (FIG's) produced at Schott Fiber Optics. These bundles have been traditionally used in medical imaging systems and

remote inspection devices such as flexible endoscopes. Arrays of fiber cores are arranged in a hexagonal lattice shown in the inset of Figure 1. Fiber diameters typically range from 8 to 20 microns yielding core densities of two to fifteen thousand cores per square millimeter. Although the core-to-core alignment tolerances are less constrained than optical ribbon cables and core-per-channel arrays, the relative spatial position of each fiber within the lattice is maintained throughout the length of the bundle in order to preserve the imaging properties.

Individual fibers of the FIG are fabricated using a rod-in-tube method. In this technique, a solid core glass is surrounded by a cladding tube to create the individual waveguide structure. The cladding is then surrounded by a second tube of acid-soluble glass (ASG). This three glass system is drawn down into a single mono fiber that is stacked into a hexagonal array, called a multi-assembly. This multi-assembly is further drawn down into a multi rod. A second stacking and drawing operation follows to create a multi-multi rod. Throughout these draws, the glasses maintain their shape, preserve the core/clad boundaries, and reduce any manufacturing variances in the original mono fiber. The ASG fuses together during the draw, locking the waveguides into the designed lattice. The multi-multi rods, which are rigid at this point, are cut and polished to the appropriate length. Prior to placing the bundle in an acid bath, the ends of each bundle are encased in wax. The acid dissolves the ASG in the middle of the bundle while the wax protects the ASG at the ends. After the wax is removed, the central part of every fiber is free to flex.

Rigid guides can also be manufactured by omitting the ASG layer, thus increasing the effective core transmission area.

Experiment 1: Transmission of a Dense Spot Array

Our first experiment was designed to test channel resolution in a dense spot array. The optical channels consisted of a 6x10 array of static spots generated by a computer generated hologram spot array generator. The spot array generator was designed to have an asymmetric spot pitch such that the pitch in Y direction was twice that of the X direction. A collimated, 855 nm, laser beam was used to illuminate the spot array generator. Bulk optics was used to image the spot array with a spot pitch of 62.5um by 125um on the input surface of the fiber bundle. This spot pitch was chosen based on specifications of the fiber bundle selected which had 11um fiber core fibers on a 15um pitch. Thus a spot of size of 35um, equal to approximately 50% of the spot pitch (in the x direction) would be transmitted in at least 4 cores, two cores aligned in each direction. Figure 2 is the CCD camera image of the spot array at the output of the fiber bundle. In this image, the individual spots are slightly larger than expected but are clearly resolvable. This implies that some channels are probably being at least partially transmitted by as many as 7 cores with as few as one dark core separating each spot in the 62.5um micron pitch direction.

Experiment 2: Butt Coupling to VCSEL Array

In our second experiment, the fiber bundle was butt coupled to a 2D VCSEL array source. The VCSELs were 4x4 array devices obtained from Honeywell through the GMU co-op program[4]. Spot pitch for these devices was 250um with each device having a 15um aperture and divergence angle of 15 degrees. The VCSELs were individually modulated through a series resister by the output from of a Tektronix Model DG2020 word generator. Figure 3 shows a photograph of the fiber bundle butt coupling mechanism. The rigid end of the fiber bundle is shown in the center being held in close proximity to the surface of the VCSEL array be a clamp mounted on an XYZ stage. There were no other optical elements between the fiber bundle and the surface of VCSEL array chip. The numerical aperture of the fiber cores was sufficiently large to capture the beam over a wide range of coupling distances. As expected, output spot size varied based on coupling distance. There was a tendency for the edges of each spot to blur at longer coupling distances when larger numbers of cores became partially filled. However, we were easily able to obtain sharply defined spots of approximately 85um diameter. Based on the divergence and aperture specifications for the lasers, this implies that the end of the fiber was positioned at approximately 125 microns from the laser aperture. Figure 4 is a frame sequence showing various modulation patterns on the array output at this coupling distance.

Experiment 3: 16 Channel point to point interconnection

After successfully coupling VCSEL sources to the fiber bundles, our next experiment tested a complete multichannel chip-to-chip interconnect. The VCSEL chips obtained from Honeywell were designed for such a setup as they include arrays of VSCEL sources and Metal-Semiconductor-Metal (MSM) detectors interleaved in a 4x4 array on the same substrate. The interleaving pattern, shown in Figure 5, is arranged such that two devices can be set up with complementary devices aligned by a 180 degree rotation followed by a 125um (1/2 pitch) shift along each axis. In our case, it was not necessary to physically rotate and shift the devices. Instead, we performed these transformations by changing the relative orientation of the two ends of the fiber bundle.

Each of the MSM detectors was biased at 7.5 volts through a series resistor and the output recorded on a digital oscilloscope. As in the previous experiment, the output from the word generator was used to simultaneously modulate independent data onto each VCSEL. The MSM output for each channel is shown in Figure 6. Channel bandwidth was limited to 250Khz by the device packaging, discrete components and wiring in the electronic setup. Optical power and detector integration time was not a limit since published results for the VCSEL and MSM devices usedconfirm operation well in excess of 1 GHz[5]. Also, one of the channels shown in

Figure 6 is not operational due a broken bonding wire that resulted from a previous alignment mishap.

Crosstalk between the channels was measured in a second experiment in which two of the four center channels in the array were kept active while all other channels were turned off. The output of this configuration is shown in Figure 7. Measured output at the detectors for the inactive channels shows maximum channel crosstalk of -23db.

Experiment 4: Optical Power Loss Characteristics

Optical power budget is a significant issue on a optoelectronic interconnection link. In our fourth experiment we attempted the characterize the relative contributions of insertion and transmission losses for fiber bundles of various lengths and fill factors. We tested end-to-end loss by lauching a single 500 micron spot at 1mW of power and measuring the output as a function of length and core/cladding fill factor. Fiber bundle lengths of 5, 20, and 40 inches were tested as well as fill factors of approximately 50% and 75% .

These tests showed that the dominant loss mechanism was by far the insertion loss. Insertion loss measurement closely tracked the fill factor to two fiber bundles tested. In each case we observed optical power loss through the fiber bundle within 3 to 5 percent of the specified fill

factor. We were not able to observe significant variations in transmission loss versus over the 35 inch range tested.

Power uniformity across the surface of the fiber bundle was also tested by scanning a 200 micron spot across the surface of a test bundle and measuring output power as a function of spot position. The results are shown in Figure 8. The majority of the surface was found to be uniform to within 1% except for a few small defects near the edges which showed variances of up to 2%.

Experiment 5: Passive Spatial Switching

In addition to point-to-point interconnections, a variety of specialized interconnection structures can be fabricated using imaging fiber bundles. For our final experiment we designed and tested one such structure, a passive spatial switch. This switch is diagrammed in Figure 9. It consists of two stacks of rectangular imaging fiber bundles. Each stack is fabricated by bonding a set of bundles at one end while coupling the other end to an OE chip. The bonded end of each stack is then bonded end-to-end with a 90^{o} relative rotation. Figure 9 is a 3 x 3 implementation in which three bundles are stacked and bonded vertically on the left side of the diagram and three more are stacked and bonded horizontally on the right side of the diagram.

The resulting structure provides for spatially resolved bi-directional channels within the fiber bundles at the loose end, presumably coupled to an OE chip. For example, consider the top fiber

bundle in the vertical stack on the left side of Figure 9. Optical channels imaged on to the left third of this bundle, represented by the arrow labeled A, are coupled into a corresponding region of the left fiber bundle in the horizontal stack. Channels imaged on middle third, represented by the arrow labeled B, are transmitted to the middle bundle in the horizontal stack and correspondingly channels imaged on the right region, represented by the arrow labeled C, are coupled to the right bundle in the horizontal stack. Moreover, channels from each of the bundles in the vertical stack exit the corresponding bundles in the horizontal stack within a specific region and are thus spatially identifiable. Since imaging fiber bundles are bi-directional, this structure can implement either a 3 to 3 bi-directional crossbar or, if the loose ends of each of the horizontal and vertical stacks are pair-wise bonded and coupled to single devices, a 3x3 full interconnect.

To test the basic optical properties of this a structure, a 3 x 3 test element was built by bonding six rigid rectangular fiber bundles in the manner described above. A photograph of this structure is shown in Figure 10. Since there were no “loose ends” in this test structure, a flexible bundle was butt coupled on one of the input surfaces and the other end coupled to a VCSEL array for testing. This bundle can clearly be seen in Figure 10 as the dark hexagonal structure at the center of the top row. The excess material shown above the top is an overlap caused by the mismatch in the aspect ratio the stacks. The active region is the 3x3 array on the bottom formed by the

intersection of the horizontal and vertical stacks. From this photograph it can be seen that individual spots are clearly resolvable through this structure even thought the spots have crossed two coupling boundaries for which no attempt was made to align the fiber cores.

Summary and Conclusions

In the five experiments described in this paper we have demonstrated and characterized the basic functionality of imaging fiber bundles for chip level interconnections. We demonstrated spot density on the order of twice the core pitch of a fiber bundle. We have shown that OE integrated circuits including sources and detectors can be directly butt coupled to fiber bundles without any additional optical elements. We have demonstrated a 16 channel interconnect with –23db of crosstalk and we have identified the most significant optical loss mechanism. Finally, we have demonstrated a basic example of a hybrid bonded structure that implements a low cost high connectivity solution for more advanced system architectures.

Acknowledgements

Authors Chiarulli and Levitan were supported, in part, by AFRL/Rome contract F30602-96-C-0206. The authors also wish to acknowledge the support of Schott Fiber Optics Inc. and the Consortium for Optical and Optoelectronic Technologies in Computing for devices and foundry services.

References

1 D. Chiarulli, S. Levitan., P. Derr, R. Menon, N. Wattanapongsakorn, Bryan. Greiner, and.M. Robinson, *Multichannel Optical Interconnections using Imaging Fiber Bundles,* in *Optics in Computing*. 1999, Optical Society of America: Washington DC. p. 112-115.

2. D. Chiarulli, S. Levitan., R. Melhem, J. Teza and G. Gravenstreter, *Partitioned Optical Passive Star (POPS) Interconnection Networks with Distributed Control.* IEEE Journal on Lightwave Technology;, 1996. **14**(7): p. 1601-1612.

3. A.A. Sawchuck, B.K.J., C.S. Raghavendra, and A. Verma, *Optical Crossbar networks.* IEEE Computer, 1987. **20**(6): p. 50-60.

4. *http//co-op.gmu.edu*

5. Liu, Y., *Smart Pixel Module Development for Free Space Optical Interconnect*, in *Optics in Computing*, D.M. P. Chavel, H. Thienpont, Editor. 1998. p. 528-531.

Figure Captions

Figure 1: FIG Cores in hex lattice with 11 micron spots on 15 micron pitch.

Figure 2: 2mm fiber Bundle output of 6x10 (62.5 x 125micron pitch) spot array.

Figure 3: Photograph of Fiber Bundle butt coupled to OE chip.

Figure 4: Frame Sequence of butt coupled 4x4 VCSEL array output.

Figure 5: Point-to-point VCSEL array setup showing interleaved source/detector arrays.

Figure 6: Data output from 16 channel interconnect.

Units: millivolts versus microseconds

Figure 7: Crosstalk test for 16 channel link.

Units: millivolts versus microseconds

Figure 8: Transmitted Optical Power versus XY position for 200micron spot.

Figure 9: 3x3 passive switch.

Figure 10: 3x3 core element.

Figure 1:

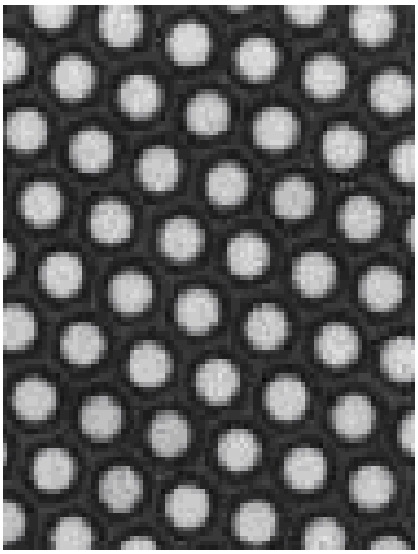

Figure 2:

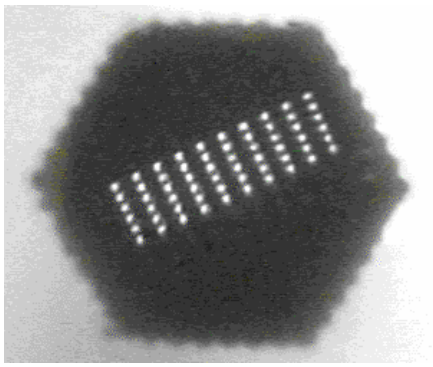

Figure 3:

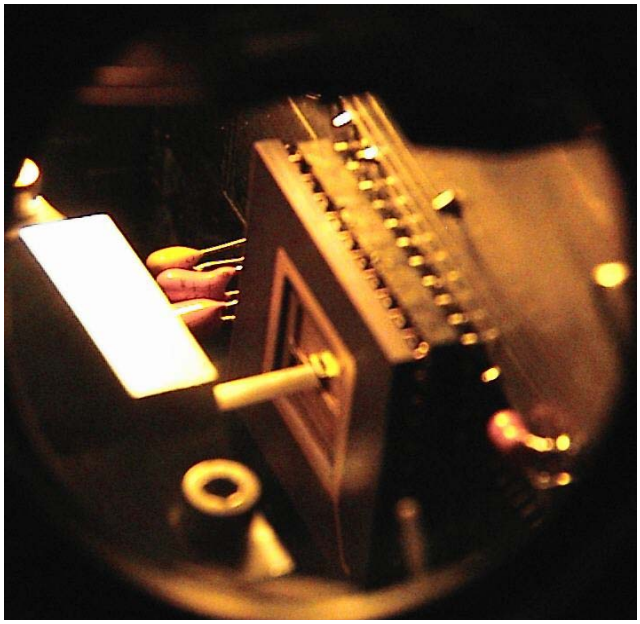

Figure 4:

Figure 5:

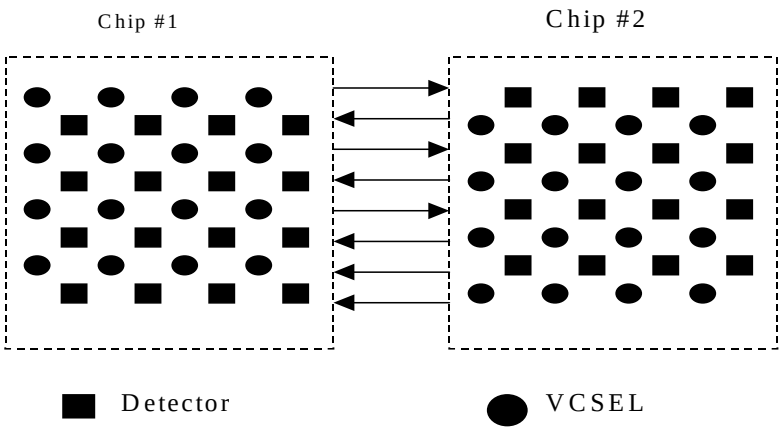

Figure 6:

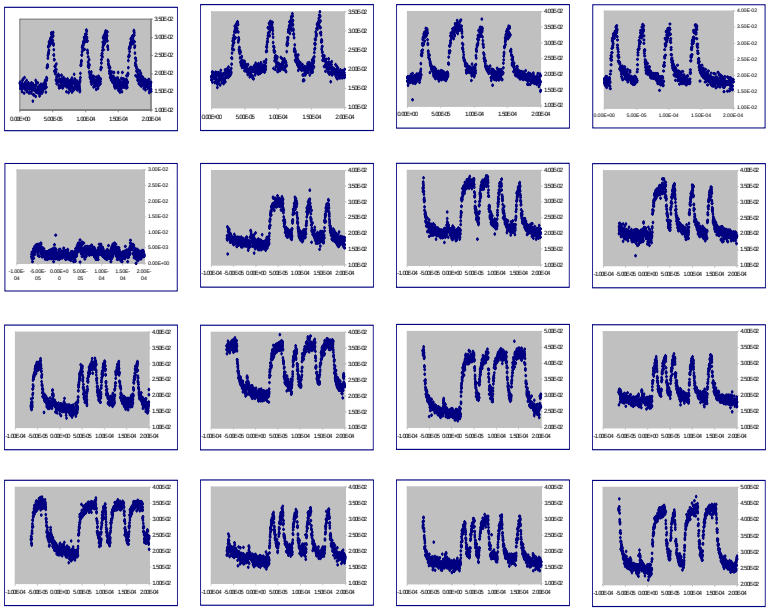

Figure 7:

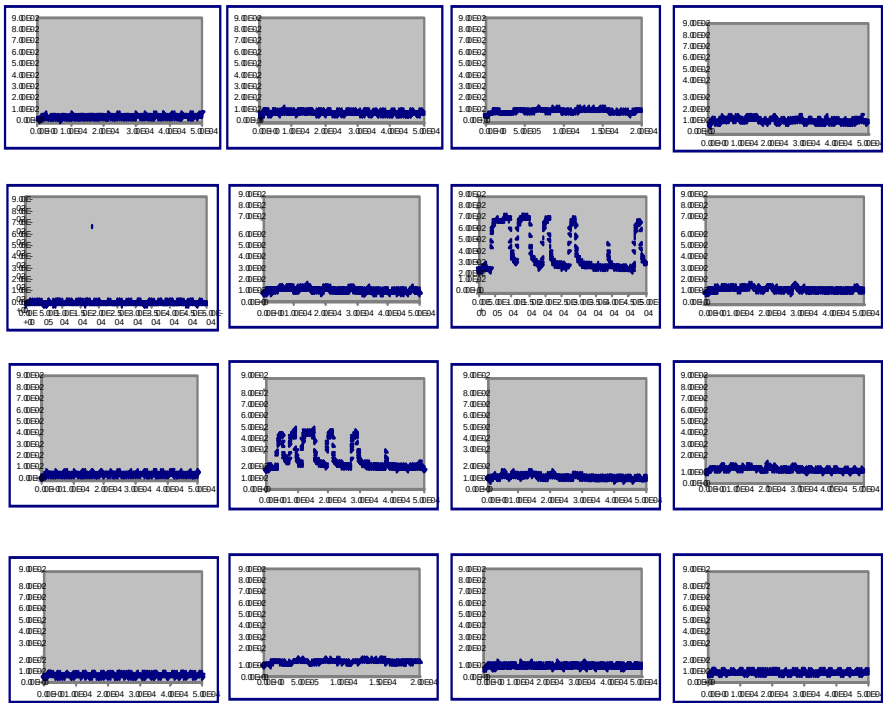

Figure 8:

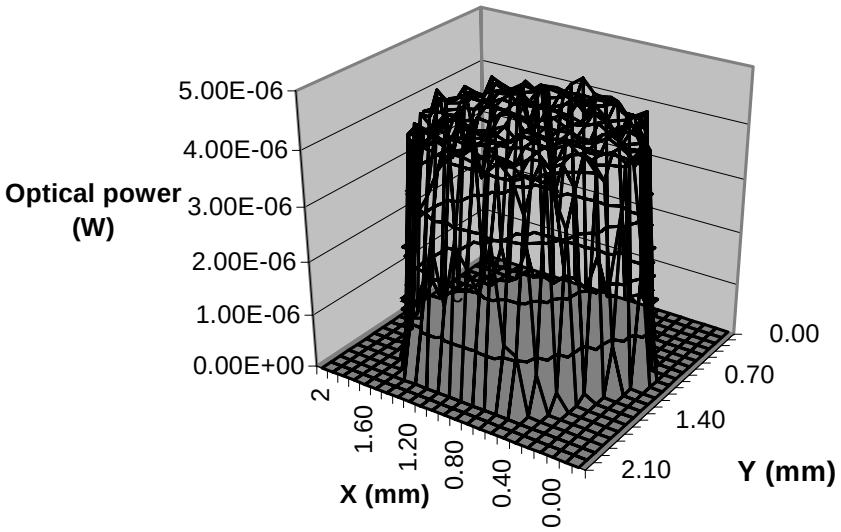
Optical power (W)
5.00E-06
4.00E-06
3.00E-06
2.00E-06
1.00E-06
0.00E+00
2
1.60
1.20
0.80
0.40
0.00
X (mm)
0.00
0.70
1.40
2.10
Y (mm)

Figure 9:

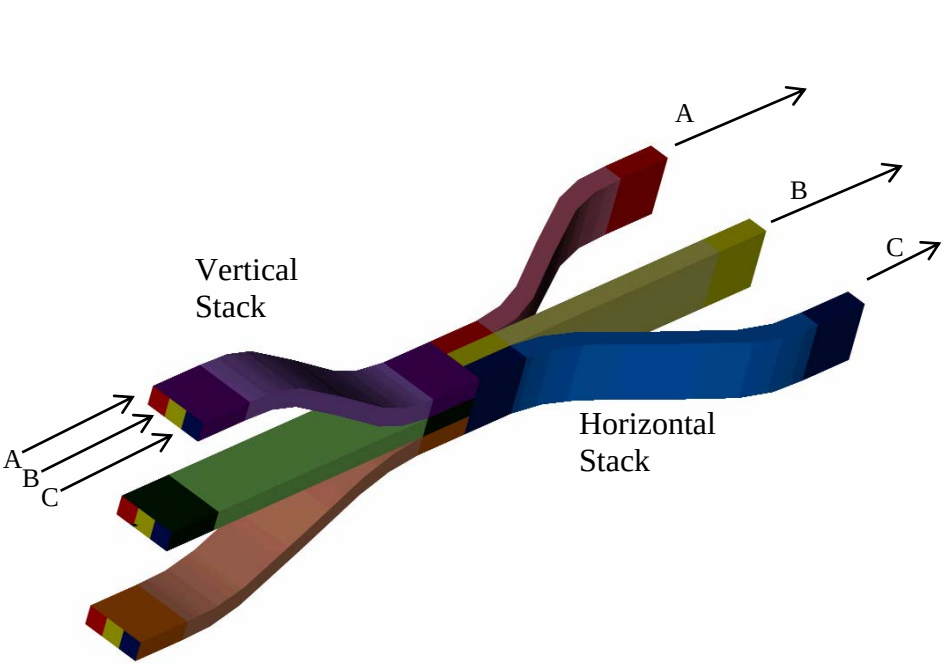

Figure 10: